JOURNAL OF APPLIED ELECTROCHEMISTRY 13 (1983) 775–782

The mechanism of spongy electrodeposits formation on inert substrate at low overpotentials

K. I. POPOV, N. V. KRSTAJIĆ*

*Faculty of Technology and Metallurgy and *Institute for Electrochemistry ICTM, University of Beograd, Beograd, Yugoslavia*

Received 3 March 1983

The mechanism of formation of spongy deposits on inert substrates at low overpotentials is discussed.

Nomenclature

C_0	bulk concentration
D	diffusion coefficient
F	Faraday constant
f	$\exp(\eta/\eta_{o,c}) - \exp(-\eta/\eta_{o,a})$
f_1	$\exp(\eta/\eta_{o,c})$
f_2	$\exp(-\eta/\eta_{o,a})$
i_0	exchange current density
i	current density
i_L	limiting current density
$i_{L,S}$	limiting current density under spherical diffusion control
n	number of electrons
N	number of nuclei (cm^2)
r	radius of growing nucleus
r_0	radius of critical nucleus
r_c	radius of growing nucleus at which deposition becomes mixed controlled
t	time
t_i	induction time for spongy growth initiation
V	molar volume
γ	surface energy
δ	thickness of diffusion layer
$2{,}3\eta_{o,c}$	slope of cathodic Tafel line
$2{,}3\eta_{o,a}$	slope of anodic Tafel line

1. Introduction

It is known that two kinds of disperse deposits can be formed during prolonged deposition: spongy at low and dendritic at high deposition overpotentials [1]. The mechanisms of dendrite growth and dendrite initiation were quantitatively described in recent papers [2–4] and a number of other papers also deal with it [5–8]. In contrast, the mechanism of spongy deposit formation has not been treated quantitatively, although some qualitative aspects have been considered [3, 9–15]. The purpose of this work is to discuss some further aspects of this phenomenon.

2. Experimental details

The electrolytes used throughout this work were 0.1 mol dm^{-3} zincate solution in 1 mol dm^{-3} KOH for the electrodeposition of zinc and 1 mol dm^{-3} $CdSO_4$ + 0.5 mol dm^{-3} H_2SO_4 and 0.005 mol dm^{-3} $CdSO_4$ + 0.4 mol dm^{-3} K_2SO_4 + 0.1 mol dm^{-3} H_2SO_4 for the electrodeposition of cadmium. The solutions were prepared from AR grade reagents and triple-distilled water. Concentrated zincate stock solution was made by dissolving ZnO in concentrated CO_2-free KOH solution at 80 to 90° C, in a flask under reflux in a nitrogen atmosphere. After dilution, the solution was analysed for zinc by EDTA-titration and for KOH by acidimetric titration. All experiments were carried out in a three compartment glass cell at 25° C, with tube for bubbling nitrogen.

Zinc and cadmium were deposited onto a stationary vertical copper cathodes. Prior to each experiment the surface of the electrode was mechanically polished with silicon carbide paper (grits 180, 320 and 600) and then with alumina powders (1.0 and 0.3 μm) and etched in 80% H_2SO_4 solution. The electrode was held in a Teflon holder exposing only the surface to be polished. The counter electrode was a high purity (99.99%) zinc plate for experiments with zinc and a high purity (99.99%) cadmium plate for those

0021–891X/83 $03.00 + .12

with cadmium. The reference electrodes were a Hg/HgO and a saturated mercurous sulphate electrode connected to the Luggin capillary via a salt bridge of the test solution.

The experiments consisted of setting the electrode at a constant potential, negative to the reversible potential of zinc or cadmium, by means of a Wenking potentiostat, for a chosen period of time. A PAR-175-programmer and Tektronix (type 564B) oscilloscope were employed to determine the Ohmic drop correction. After a period of deposition, the electrode was taken out of the cell,

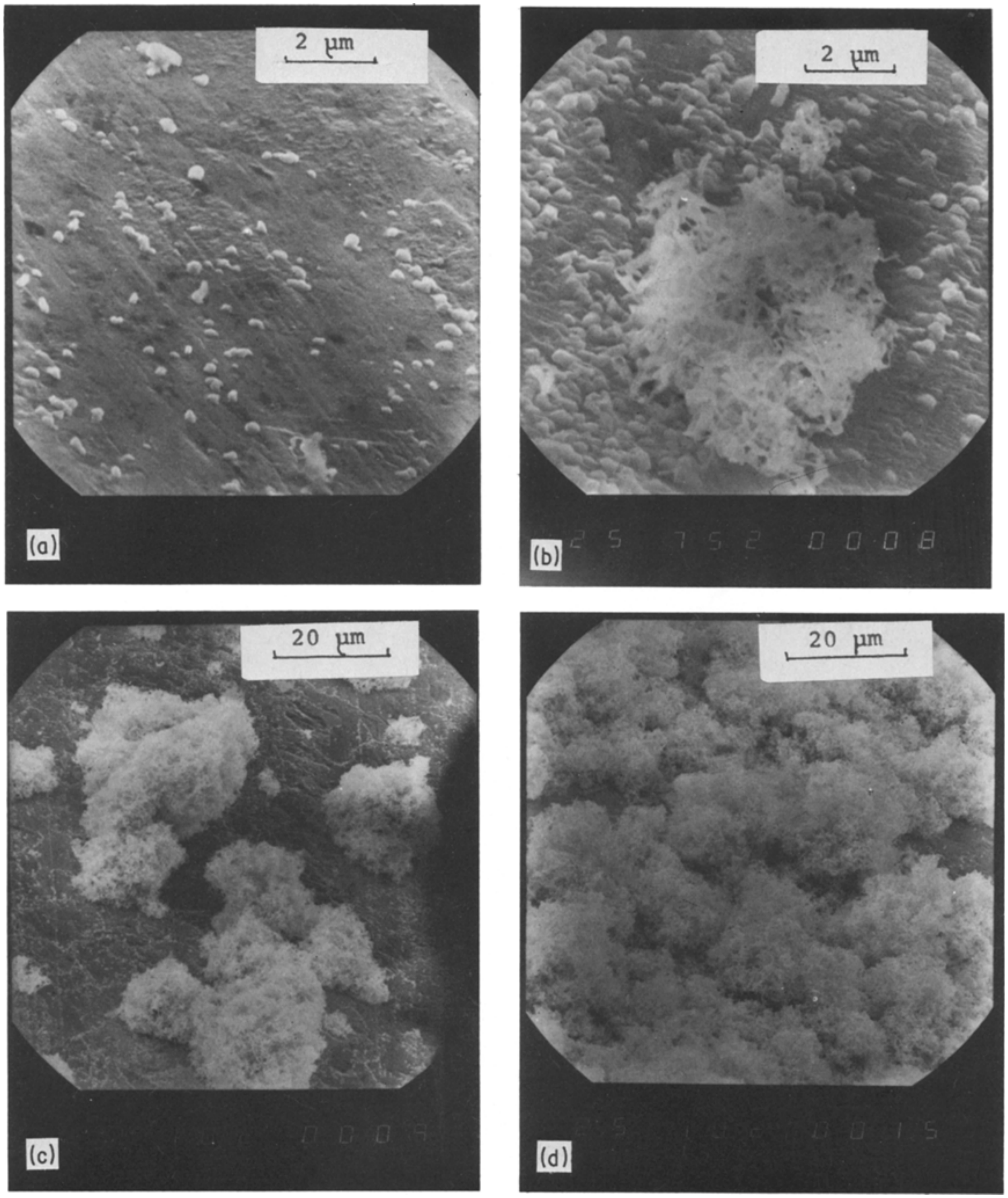

Fig. 1. Zinc deposits at 20 mV from 0.1 mol dm^{-3} zincate and 1 mol dm^{-3} KOH solution. (a) 10 min SEM, 60°, × 6450. (b) 20 min SEM, 60°, × 6450. (c) 30 min SEM, 60°, × 860. (d) 60 min SEM, 60°, × 860.

washed and dried. The morphology of the deposits was investigated by scanning electron microscopy.

3. Results and discussion

The SEM pictures of zinc deposited at overpotentials of 20 and 100 mV as a function of deposition time, are presented in Figs. 1 and 2, respectively. It is seen that a spongy deposit is formed at 20 mV, and dendritic one at 100 mV. This is in accordance with the literature [3, 9–11].

It is known that at constant overpotential the number of nuclei increases with pulse duration, tending to a saturation value at higher durations. At the same time the saturation values, i.e. the maximum number of nucleation sites which can be occupied increases with overpotential [16].

At high overpotentials, many nuclei are formed, resulting in a rapid formation of a compact surface film of metal. In this case the system behaves similarly to when the deposition is onto zinc itself [4]. It is seen from Fig. 2a that after 5 min at 100 mV, the inert substrate is completely covered in deposit and dendritic growth has begun. During prolonged deposition, classical flat dendrites [10, 11] are formed, see Fig. 2b. Deposits of this kind were obtained at overpotentials larger than 80 mV.

The formation of spongy deposits can be explained in the following way:

The relation between η and i is given by

$$i = \frac{i_0[\exp(\eta/\eta_{o,c}) - \exp(-\eta/\eta_{o,a})]}{1 + \frac{i_0}{i_L}\exp(\eta/\eta_{o,c})} = \frac{i_0(f_1 - f_2)}{1 + \frac{i_0}{i_L} f_1} \qquad (1)$$

Obviously, at low overpotentials, the form of the deposit is determined by the i_0/i_L ratio. Deposition will be activation controlled if

$$\frac{i_0}{i_L} \ll 1 \qquad (2)$$

and diffusion controlled if

$$\frac{i_0}{i_L} \gg 1 \qquad (3)$$

At low overpotentials small numbers of nuclei are formed and they grow independently, see Fig. 1a.

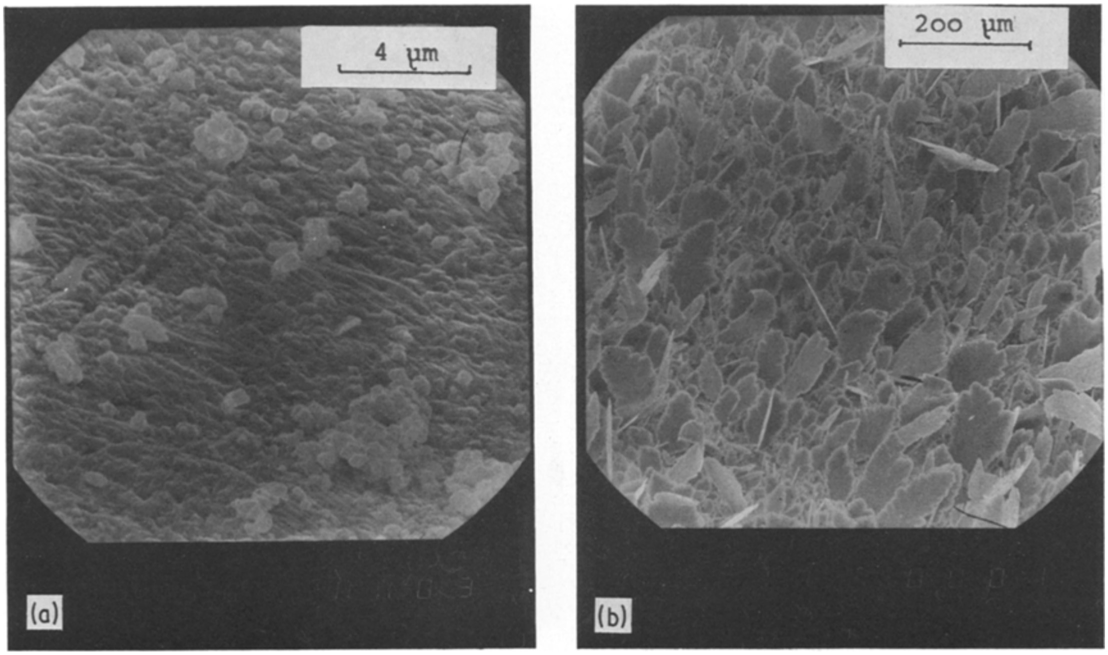

Fig. 2. Zinc deposits at 100 mV from 0.1 mol dm^{-3} zincate and 1 mol dm^{-3} KOH solution. (a) 5 min SEM, 60°, × 4300. (b) 60 min SEM, 60°, × 86.

The diffusion limited current to the growing nucleus is given by

$$i_{\mathrm{L,s}} = \frac{nFDC_0}{r} \tag{4}$$

or

$$i_{\mathrm{L,s}} = \frac{i_{\mathrm{L}}\delta}{r} \tag{5}$$

It can be assumed that the process enters mixed activation – diffusion control at

$$i \geqslant 0.2 i_{\mathrm{L}} \tag{6}$$

and by combining Equations 1, 5 and 6, one obtains,

$$r_{\mathrm{c}} = \frac{i_{\mathrm{L}}}{i_0} \frac{\delta}{4f_1 - 5f_2} \tag{7}$$

the value of the radius of the growing nucleus when the process becomes mixed controlled. The critical radius at overpotential η is given by

$$r_0 = \frac{2\gamma V}{nF} \tag{8}$$

being extremely low even at low overpotentials [17].

The radius of growing nucleus will vary with time according to [18]

$$r = r_0 + \frac{V}{nF} i_0 ft \approx \frac{V}{nF} i_0 ft \tag{9}$$

and by combining Equations 7 and 9, it can be shown that r_{c} will be reached at

$$t_{\mathrm{i}} = \frac{i_{\mathrm{L}}}{i_0^2} \frac{nF\delta}{Vf(4f_1 - 5f_2)}. \tag{10}$$

In this situation, amplification of the surface roughness, or rather, of surface irregularities on the growing nucleus takes place [1, 19], just as in the case of deposition onto stationary wire electrodes in mixed or diffusion control. (See Fig. 2 from [20]; plate 1 from [21], and Fig. 6 from [22].) Once initiated, the amplification of surface protrusions lead to the formation of the spherical aglomerate of filaments, which form spongy deposits [10]. This discussion is illustrated by Figs. 1a and 1b. It is also seen from the same figures that in this system, 10 min $< t_{\mathrm{i}} <$ 20 min. The estimated value of $t_{\mathrm{i}} \approx 2$ min at $\eta = 20$ mV using Equation 10 and $i_{\mathrm{L}} = 10^{-2}$ A cm^{-2}, $i_0 = 10^{-1}$ A cm^{-2}, $2.3\eta_{\mathrm{o,c}} = 120$ mV dec^{-1}, $2.3\eta_{\mathrm{o,A}} = 40$ mV dec^{-1} [3, 5], $\delta = 2 \times 10^{-2}$ cm, and $V = 9.15$ cm^3 mol^{-1}, is in a relatively good agreement with experiment.

The coverage of the electrode surface by spongy deposits increases with deposition time up to full coverage, as seen from Figs. 1c and 1d. This kind of deposit is obtained in the present work up to an overpotential of 40 mV. It is evident that spongy deposit formation by the proposed mechanism is only possible with relatively high i_0 values.

It was found in this work that in the overpotential range 40 mV $< \eta <$ 80 mV, a compact deposit is formed during a relatively long induction time, after which spongy or dendritic, or both kinds of deposits are developed on the electrode, as shown in Fig. 3. This situation, probably the same as in the case of deposition on the same substrate, was beyond the scope of this work.

Similar situations arise in cadmium deposition from 0.005 mol dm^{-3} CdSO$_4$ in a sulphate medium, as can be seen from Fig. 4. At low overpotentials spongy deposits are formed (Figs. 4a and b) and dendrites at higher ones (Fig. 4c). In the deposition of cadmium from 1 mol dm^{-3} CdSO$_4$, the situation is quite different, as can be seen from Figs. 5 and 6. After small deposition

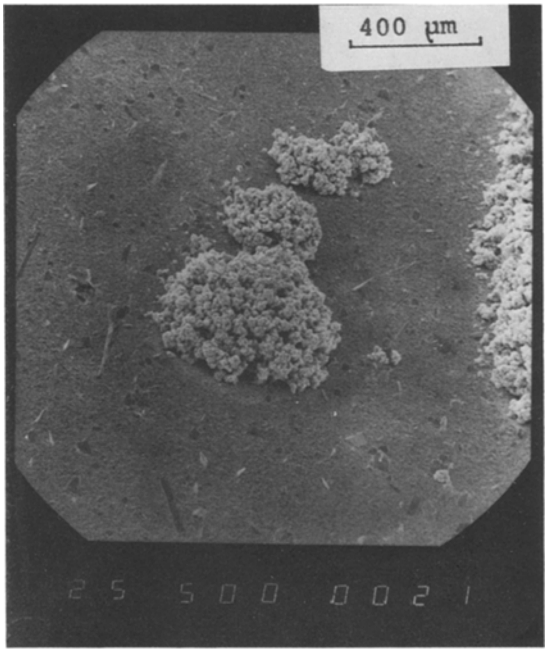

Fig. 3. Zinc deposit at 60 mV from 0.1 mol dm^{-3} zincate and 1 mol dm^{-3} KOH solution after 270 min SEM, 60°, ×43.

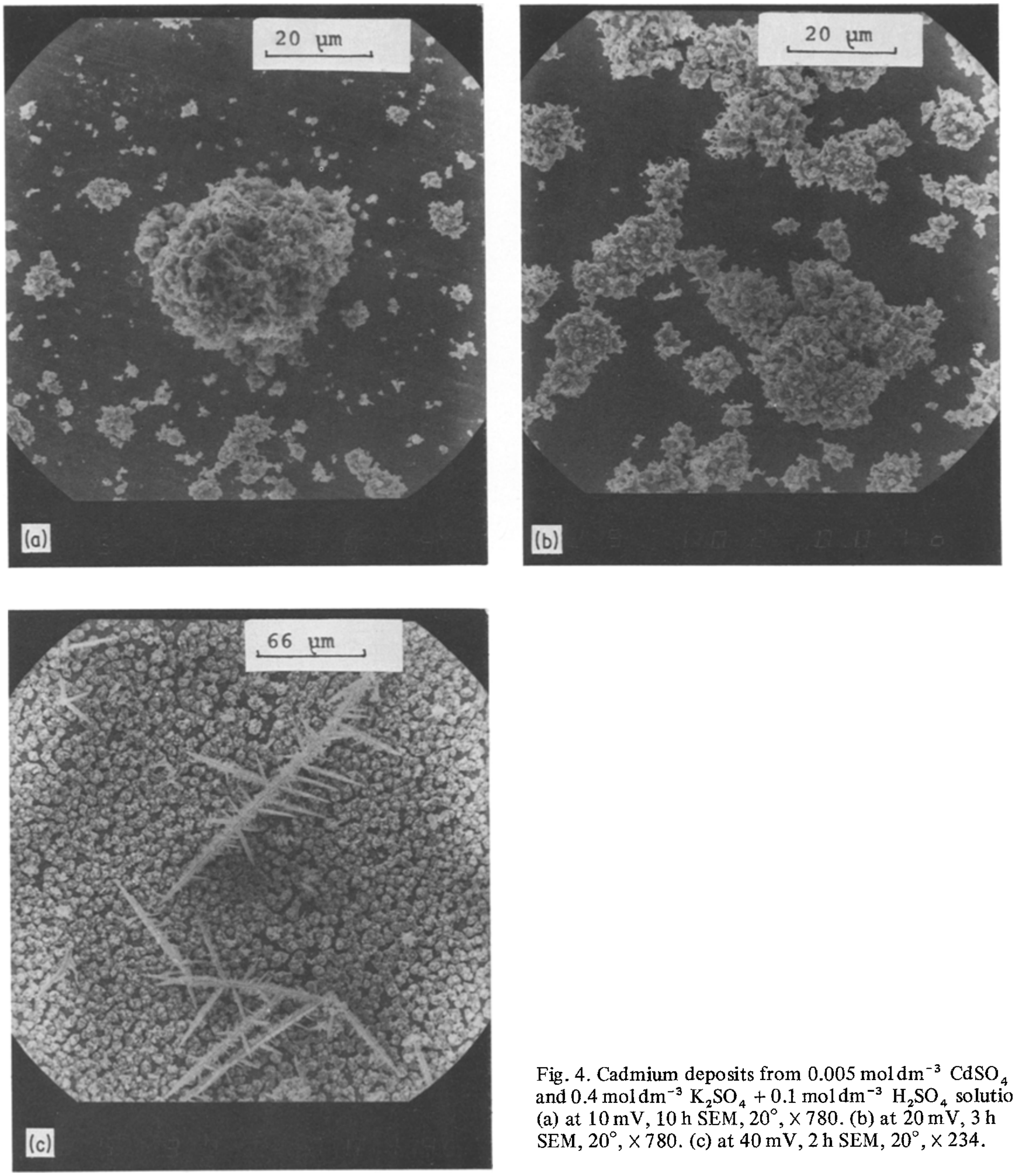

Fig. 4. Cadmium deposits from 0.005 mol dm^{-3} $CdSO_4$ and 0.4 mol dm^{-3} K_2SO_4 + 0.1 mol dm^{-3} H_2SO_4 solution. (a) at 10 mV, 10 h SEM, 20°, × 780. (b) at 20 mV, 3 h SEM, 20°, × 780. (c) at 40 mV, 2 h SEM, 20°, × 234.

times, grains with well defined crystal planes are formed (Fig. 5); at high deposition times, crystalline deposits are obtained (Fig. 6). This can be explained in the following way. According to Lorenz [23], for cadmium deposition from sulphate solution, the characteristics are $2.3\eta_{o,c}$ = 60 mV dec^{-1}, $2.3\eta_{o,a}$ = 50 mV dec^{-1}, $i_0 \approx$ 1 mA cm^{-2} and $i_0 \approx$ 10 mA cm^{-2} for 0.005 mol dm^{-3} and 1.0 mol dm^{-3} $CdSO_4$, respectively. Corresponding limiting diffusion currents can be assumed to be ≈ 0.5 mA cm^{-2} and 100 mA cm^{-2} if $\delta \approx 2 \times 10^{-2}$ cm and $D = 10^{-5}$ cm^2 s^{-1}. Using these data, η = 10 mV, V = 13 cm^3 mol^{-1} and Equation 10, it is easy to calculate that in both cases t_i is of the order of 20 h. This is in relatively good agreement with experimental findings in deposition from 0.005 mol dm^{-3} $CdSO_4$ (Fig. 4a), and in disagreement with results obtained in

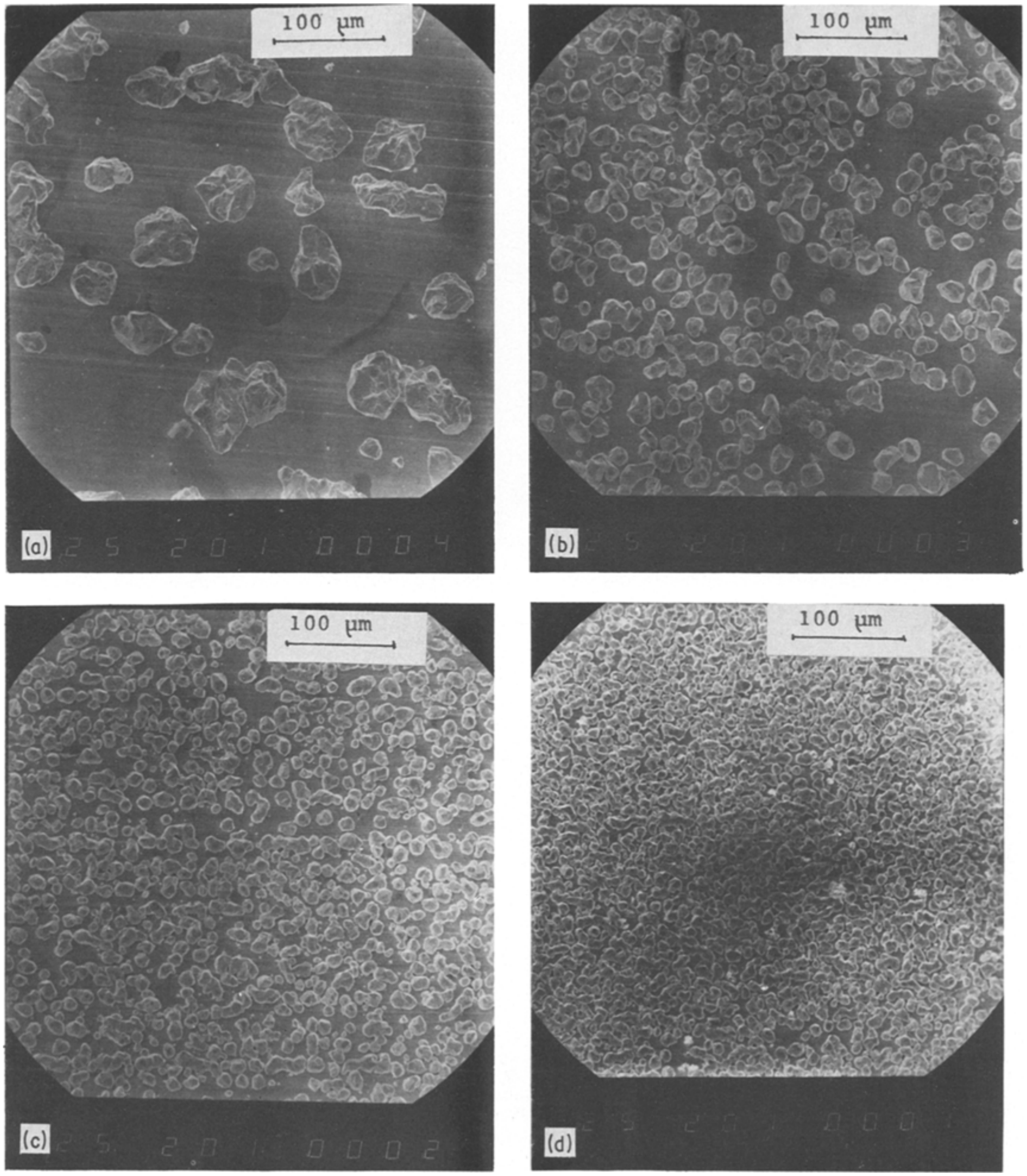

Fig. 5. Cadmium deposits from 1.0 mol dm^{-3} $CdSO_4$ and 0.5 mol dm^{-3} H_2SO_4 solution. (a) at 10 mV, 24 min SEM, 20°, × 156. (b) at 40 mV, 4 min SEM, 20°, × 156. (c) at 60 mV, 2 min SEM, 20°, × 156. (d) at 110 mV, 1.33 min SEM, 20°, × 156.

deposition from 1.0 mol dm^{-3} $CdSO_4$ (Figs. 5a and 6a). This is due to the following facts. It is easy to calculate using Equation 7 and appropriate constant that

$$r_c \approx \delta \tag{11}$$

and

$$r_c \approx 20\delta \tag{12}$$

for deposition from 0.005 mol dm^{-3} $CdSO_4$ and 1.0 mol dm^{-3} $CdSO_4$, respectively. Assuming that around each grain with radius r, growing under spherical diffusion control, a diffusion layer of the same thickness is formed, it is obvious that this condition is fulfilled if

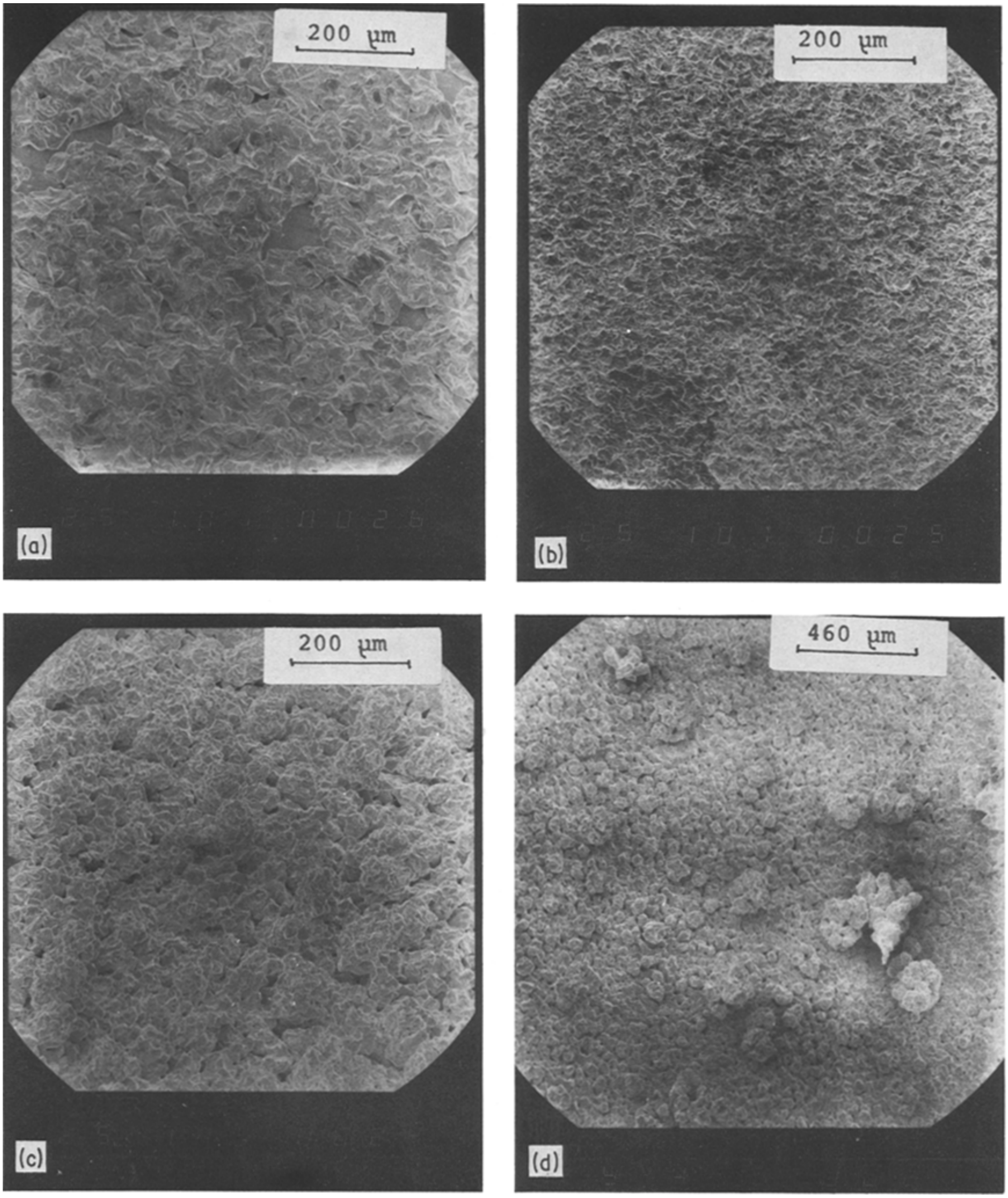

Fig. 6. Cadmium deposits from 1.0 mol dm^{-3} CdSO$_4$ and 0.5 mol dm^{-3} H$_2$SO$_4$ solution. (a) at 10 mV, 10 h SEM, 60°, × 86. (b) at 40 mV, 2.0 h SEM, 60°, × 86. (c) at 70 mV, 1.0 h SEM, 60°, × 86. (d) at 110 mV, 30 min SEM, 60°, × 37.

$$N \leqslant \frac{1}{(4r_c)^2} \qquad (13)$$

Hence, for deposition from 0.005 mol dm^{-3} CdSO$_4$

$$N \leqslant 150$$

and for deposition from 1.0 mol dm^{-3} CdSO$_4$

$$N \leqslant 0.4.$$

The nucleation rate in the first case is sufficiently low to satisfy the condition (13), and spongy deposit formation is possible. In the latter case the nucleation rate is fast and suitable conditions for spongy deposit formation cannot be reached. Hence, the grains will grow under pure activation control until a complete surface film is not formed. The morphology of deposit is then determined by linear diffusion at higher overpotentials [1, 4] lead to formation of more or less rough deposits at lower (Figs. 6a, b and c), and dendritic deposits at higher overpotentials (Fig. 6d) after prolonged deposition.

On the basis of all above facts, it can be concluded, the spongy deposit formation on an inert substrate is caused by mass transfer limitations in conditions of low nucleation rate. Suitable conditions for spongy deposits formation arises at low overpotentials in systems where $i_L \approx i_0$ or $i_L < i_0$.

Acknowledgement

The authors would like to thank Dr M. Gantar and Miss A. Milosavljević for the microphotographs.

References

[1] A. R. Despić and K. I. Popov, *Mod. Aspects Electrochem.* 7 (1972) 199.

[2] J. L. Barton and J. O'M. Bockris, *Proc. R. Soc. London Ser. A* **268** (1962) 485.

[3] J. W. Diggle, A. R. Despić and J. O'M. Bockris, *J. Electrochem. Soc.* **116** (1969) 1503.

[4] K. I. Popov, M. D. Maksimović, J. D. Trnjančev and M. G. Pavlović, *J. Appl. Electrochem.* **11** (1981) 239.

[5] J. O'M. Bockris, Z. Nagy and A. Damjanović, *J. Electrochem. Soc.* **119** (1972) 275.

[6] J. W. Diggle and A. Damjanović, *Elektrokhimiya* 7 (1971) 1107.

[7] A. R. Despić and M. M. Purenović, *J. Electrochem. Soc.* **121** (1974) 329.

[8] R. V. Moshtev and P. Zlatilova, *J. Appl. Electrochem.* 8 (1978) 213.

[9] K. I. Popov, D. N. Keča and M. D. Andjelić, *ibid.* 8 (1978) 19.

[10] M. Froment and G. Maurin, *Electrodep. Surf. Treatment* **3** (1975) 245.

[11] F. Mansfeld and S. Gilman, *J. Electrochem. Soc.* **117** (1970) 1521.

[12] I. Epelboin, M. Ksouri and R. Wiart, *J. Electroanal Chem.* **65** (1975) 373.

[13] Ph. Aubrun, F. Wenger and R. Wiart, *J. Appl. Electrochem.* 7 (1977) 225.

[14] R. D. Naybour, *J. Electrochem. Soc.* **116** (1969) 520.

[15] *Idem, Electrochim. Acta* **13** (1968) 763.

[16] R. Kaishew and E. Budevski, *Contemp. Phys.* 8 (1967) 489.

[17] S. Toshev and I. Markov, *Electrochim. Acta* **12** (1967) 281.

[18] J. O'M. Bockris, Z. Nagy and D. Dražić, *J. Electrochem. Soc.* **120** (1973) 30.

[19] S. I. Krichmar, *Elektrokhimiya* **1** (1965) 604.

[20] A. R. Despić and K. I. Popov, *J. Appl. Electrochem.* **1** (1971) 275.

[21] K. I. Popov, D. N. Keča, S. I. Vidojković, B. J. Lazarević and V. B. Milojković, *ibid.* **6** (1976) 365.

[22] K. I. Popov, M. D. Maksimović, D. T. Lukić and M. G. Pavlović, *ibid* **10** (1980) 299.

[23] W. Lorenz, *Z. Elektrochem.* 58 (1954) 912.